Dynamic response of tunnels due to surface explosions using nonlinear numerical modelling

Ali Adnan Khadra [1], Hala Hasan [1], Turki Tabak [2]

[1] Higher Institute for Earthquake Studies and Research, Damascus University, Syria
[2] Scientific Studies and Research Center of Aleppo, Syria
ali.khadra@damascusuniversity.edu.sy hala.hasan@damascusuniversity.edu.sy

Destructive blasts can have strong effects on buried facilities. This paper evaluates the dynamic response of a reinforced concrete tunnel using one complete model, which includes an explosion, the shock wave propagation through the soil, the interaction of the soil with the tunnel lining, and the tunnel response itself. The simulations were performed using the ABAQUS/Explicit finite element package. For the explosion the Jones-Wilkens-Lee equation is used. The soil behaviour is captured with the elastoplastic Drucker-Prager Cap model, the concrete is described by the Concrete Damaged Plasticity model and the reinforcement is modelled as an elasto-plastic material. The contact surface between the soil and the tunnel uses Mohr-Coulomb friction that allows for sliding, separating, and rebounding of the tunnel's surface to the surrounding soil. Varied parameters are the reinforcement ratio and the construction depth. Increasing the reinforcement ratio reduces the, damage to the tunnel lining and with a suitable construction depth, the tunnel can be relatively safe from failure.

Keywords: Surface explosion, numerical simulation, dynamic response, soil-structure interaction, tunnel

1 Introduction

The dynamic response of buried structures can be important in structural and geotechnical engineering. These buried structures by definition are all forms of facilities that are built underground and used for civil societal purposes, such as tunnels and buried tanks, or strategic purposes, for example, military shelters and nuclear power plants. Dynamic blast analysis methods of various types; analytical, experimental and numerical, must include a

complete description of the analyses process; (1) the phenomenon of the explosion, (2) the propagation of the blast waves in the medium, (3) the response of the structure and (4) the material damage to structural elements [7, 10, 12].

Numerical methods are considered the best tools in simulating the whole system (explosion - soil - structure) due to their ease, availability and results that can be calibrated with codes of practice and research. Experimental methods are considered exclusive to specific government agencies and the reports are not available in the open literature. As for analytical methods, these are difficult to perform due to the complexity of buried facility dynamics, despite the simplifying hypotheses that can be adopted, because of the large number of calculations involved [7, 10, 12].

Tunnels can be defined as a cavities that are located under the ground surface and are used for a certain purpose [4]. The considered threat to buried facilities is a ground shock produced by an explosion on or under the ground surface near these structures. The intensity of blast loading is affected by many variables, which are: (a) weapon size and its distance to the structure, (b) depth of weapon penetration at the time of burst and (c) mechanical properties of the soil as it is the transporter medium between the detonation point and the structure, which is the least predictable factor due to wide variations of soil types [1]. Figure 1 shows possible explosions against a buried facility.

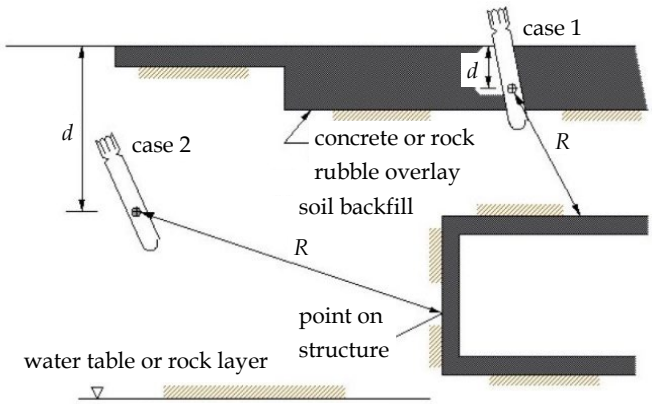

Figure 1. Possible explosions next to a buried facility [1]

In this paper, due to the serviceability importance of tunnel structures in critical events and according to previous studies [7, 10, 11, 12], a numerical model of a buried tunnel is

performed to investigate the effects of the tunnel lining reinforcement ratio and construction depth on the dynamic response of the tunnel exposed to surface explosion loads. To this end, the ABAQUS/EXPLICIT program is used to perform a parametric study with a complete coupled model (explosive - soil - tunnel) that includes nonlinear material models.

2 Numerical model

2.1 Background and finite element model

The geometry of the numerical model is based on previous reference studies [7, 10]. These studies are axisymmetric and equivalent to a buried cylindrical tank with a reinforced concrete lining. The present tunnel model is two-dimensional and plane strain. The geometric characteristics of the studied tunnel are the same as those of the cylindrical tank in terms of the shape and dimensions of the cross-section, material specifications, charge mass and interaction characteristics of the contacts.

Figure 2 shows half of the symmetrical model. The tunnel lining has a thickness t = 0.5 m, an internal height h = 3 m, and an overall width w = 8 m. The reinforcement ratio of the tunnel's concrete lining is a parameter that varies between the minimum and maximum ratios adopted by [2]. The depth of the tunnel d_i is the second parameter with two different values d_1 = 4 m and d_2 = 8 m as shown in Figure 2a. Due to the geometry of the explosion against the structure, the most critical element faces the charge [1, 10]. The explosive TNT charge has a mass of 100 kg and is positioned above the tunnel roof. The target points are (1) the tunnel roof centre, (2) the quarter-span of the tunnel roof, and (3) the corner of the tunnel roof (Fig. 2a).

The Arbitrary Lagrangian-Eulerian technique (ALE) is utilized to eliminate mesh distortion where high deformation is expected (i.e. the soil region near the explosion) [6, 10]. This technique combines the advantages of pure Lagrangian analysis and pure Eulerian analysis, which makes it possible to maintain a high-quality mesh during an analysis, for large deformations or loss of material, by allowing the mesh to move independently of the material [3]. The conventional Finite Element Method (FEM) is used for the rest of the system. The 4-node bilinear plane strain quadrilateral, reduced integration, elements (CPE4R) are used to model the entire explosive–soil–structure, while the infinite elements

(CINPE4) are used to provide quiet soil boundaries at the right-hand side and bottom of the mesh (Fig. 2b). The infinite element is shown in Figure 3 [3] and Figure 4 shows layers of soil with four infinite elements [3].

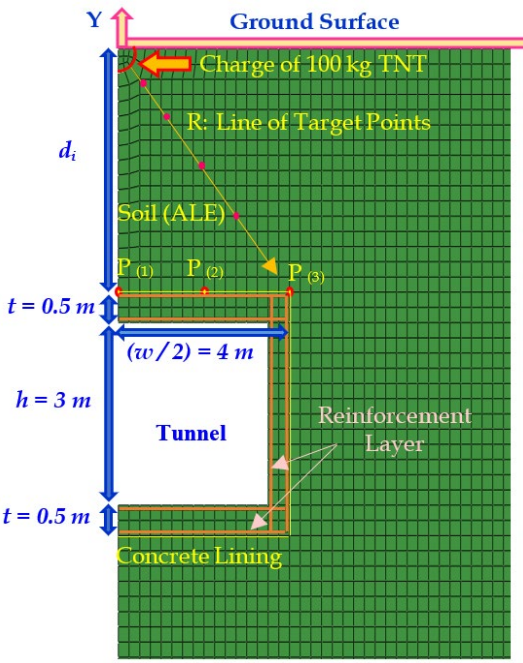

Figure 2a. Detail of the two-dimensional finite element mesh

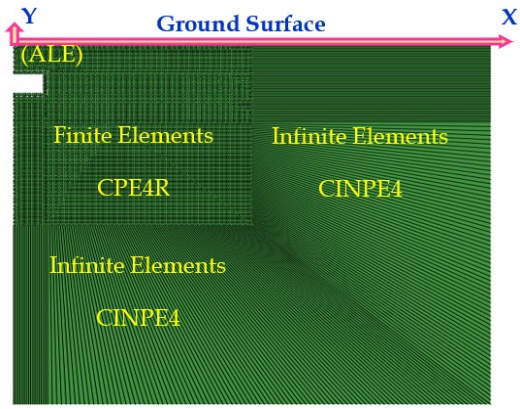

Figure 2b. Complete finite element mesh (Abaqus)

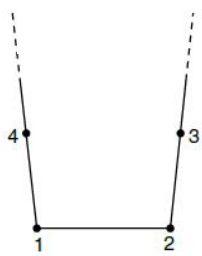

Figure 3. Abaqus Infinite element [3]

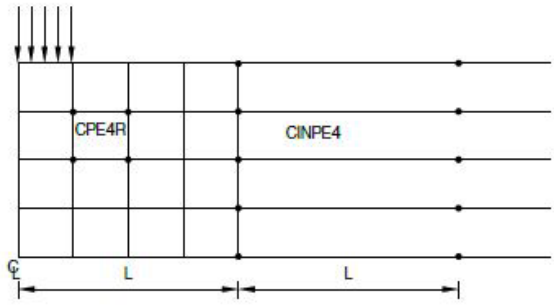

Figure 4. Layers of soil with four infinite elements [3]

2.2 *Material models and parameters*

2.2.1 *Explosive model*

The Jones-Wilkins-Lee (JWL) high explosive equation of state is used to model a TNT explosive charge. This equation expresses the pressure generated by the release of chemical energy in an explosive [3], which can be written in terms of the internal energy per unit mass E_{m0} as

$$p = A\left(1-\frac{\omega\rho}{R_1\rho_0}\right)\exp\left(-R_1\frac{\rho_0}{\rho}\right) + B\left(1-\frac{\omega\rho}{R_2\rho_0}\right)\exp\left(-R_2\frac{\rho_0}{\rho}\right) + \frac{\omega\rho^2}{\rho_0}E_{m0} \quad (1)$$

where A, B, R_1, R_2 and ω are defined as the equation coefficients, with ρ_0 being the density of the explosive and ρ being the density of the products of detonation. The initial relative density $\frac{\rho_0}{\rho}$ is assumed to be unity, which means an initial specific energy E_{m0} with nonzero values should be specified. The parameters presented in [7, 10, 11] are adopted in this study, as shown in Table 1.

Table 1. Parameters of the TNT Explosive [7, 10, 11]

parameter	value
C_d wave speed of detonation	6930 m/s
A	373800 MPa
B	3747 MPa
R_1	4.15
R_2	0.9
ω	0.35
ρ_0 explosive density	1630 kg/m^3
E_{m0} initial specific energy	3.63 J/kg

2.2.2 *Soil model*

The soil is modelled by the elastoplastic Drucker-Prager cap model. The yield surface of this model has two principal segments: a pressure-dependent Drucker-Prager shear failure segment F_s, which is a perfectly plastic yield surface (i.e. no hardening), and a compression cap segment F_c that provides an inelastic hardening mechanism. A smooth surface between the shear failure surface and cap segment is provided by a transition surface F_t, as shown

in Figure 5 [3]. The parameters for this model are adopted from [7, 11] and shown in Table 2.

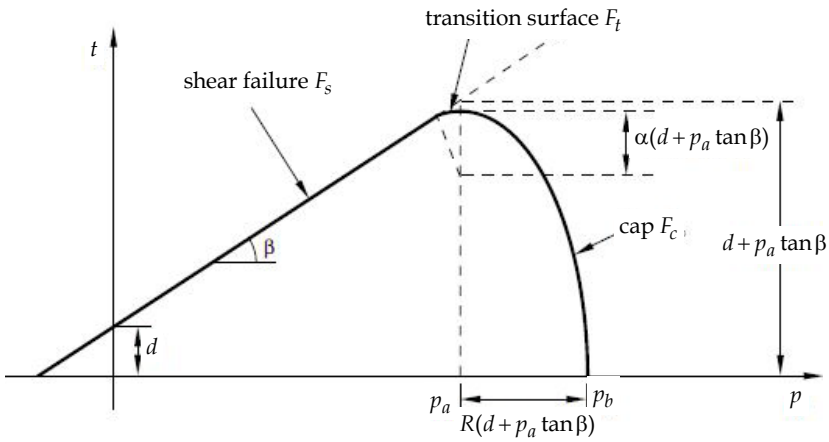

Figure 5. The Drucker-Prager cap model [3]

Table 2. Material properties of the soil [7, 11]

parameter	value
E Young's modulus	494 MPa
ν Poisson's ratio	0.17
ρ soil density	1920 kg/m^3
d material cohesion	1.38 MPa
β material angle of friction	40.4°
R cap eccentricity parameter	0.3
ξ_v initial cap yield surface position	0.02
α transition surface radius parameter	0.01
cap hardening behaviour (stress, plastic volumetric strain)	2.75 MPa, 0.00
	4.83 MPa, 0.02
	5.15 MPa, 0.04
	62.0 MPa, 0.08

2.2.3 Reinforced concrete model

Reinforcement model

The Rebar option is used to model the reinforcement layer of the tunnel lining, which has a constant thickness equal to the reinforcement area divided by the section length. The

reinforcement ratio is a parameter between a minimum and a maximum ratio adopted from [2]. The minimum ratio is $\mu_{s\min} = 0.0015$ the maximum is $\mu_{s\max} = 0.5 \frac{455}{630 + f_y} \frac{f_c'}{f_y}$ as the tunnel lining is considered a slab. The model parameters used for the reinforcement are taken from [7, 10] as Young's modulus E = 200 000 MPa, yield stress f_y = 220 MPa, steel mass density γ_{st} = 7800 kg/m^3 and Poisson's ratio ν = 0.3. The adopted thicknesses of reinforcement layers are shown in Table 3 [7], where case AS_0 is a lining without reinforcement.

Table 3. Thickness of the reinforcement layers

case	thickness of the reinforcement layer [mm]
AS_0	-
AS_1	8
AS_2	12
AS_{max}	28

Concrete model

The concrete of the tunnel lining was modelled by the Concrete Damaged Plasticity constitutive model (CDP). This model combines isotropic damaged elasticity with isotropic tensile and compressive plasticity. It is for realistic simulation of concrete behaviour in all types of structure (beams, trusses, shells, and solids). It can be used with rebar to model concrete reinforcement and in structures subjected to dynamic loading [3]. The parameters adopted for a concrete grade of B50 are adopted from [7, 10], and shown in Table 4.

2.2.4 Soil structure interaction

Simulating the contact of the structure with the surrounding soil is pivotal in this kind of dynamic problems, which can be achieved by defining the appropriate properties between the surfaces [7, 10]. Contact interaction can define tangential behaviour (friction and elastic sliding) and normal behaviour (rigid, soft, or damp contact and separation). In addition, it can contain information about damping, thermal contact, thermal radiation, and heat generation resulting from friction [3]. Thus, a formulation that allows for any arbitrary motion of the surfaces such as separation, sliding, rebound, and rotation of the surfaces in contact, has been utilized. The Coulomb friction model is used in this study, which has a

critical shear stress τ_{cr} , at which sliding of the surfaces begins, as a portion of the contact pressure. Thus, $\tau_{cr} = \mu P$, where $\mu = 0.5$ is the friction coefficient [7, 10].

Table 4. Material properties of the concrete tunnel wall [7, 10]

parameter		value	
E Young's modulus		19700 MPa	
ν Poisson's ratio		0.19	
β		38°	
ε flow potential eccentricity		1	
F_{b0}/F_{C0}		1.12	
K_C		0.666	
γ_c concrete density		2500 kg/m^3	
concrete compression hardening		concrete compression damage	
stress [Pa]	crushing strain	damage	crushing strain
15000000	0.0	0.0	0.0
20197804	0.0000747307	0.0	0.0000747307
30000609	0.0000988479	0.0	0.0000988479
40303781	0.000154123	0.0	0.000154123
50007692	0.000761538	0.0	0.000761538
40236090	0.002557559	0.195402	0.002557559
20236090	0.005675431	0.596382	0.005675431
5257557	0.011733119	0.894865	0.011733119
concrete tension stiffening		concrete tension damage	
stress [Pa]	crushing strain	damage	crushing strain
1998930	0.0	0.0	0.0
2842000	0.00003333	0.0	0.00003333
1869810	0.000160427	0.406411	0.000160427
862723	0.000279763	0.69638	0.000279763
226254	0.000684593	0.920389	0.000684593
56576	0.00108673	0.980093	0.00108673

3 Discussion and results

3.1 Soil quiet boundaries

The displacements of a point in the infinite region of the soil are investigated. These displacements have zero values when the dynamic load is active (Fig. 6). This shows that the quiet boundaries do not reflect waves back to the tunnel.

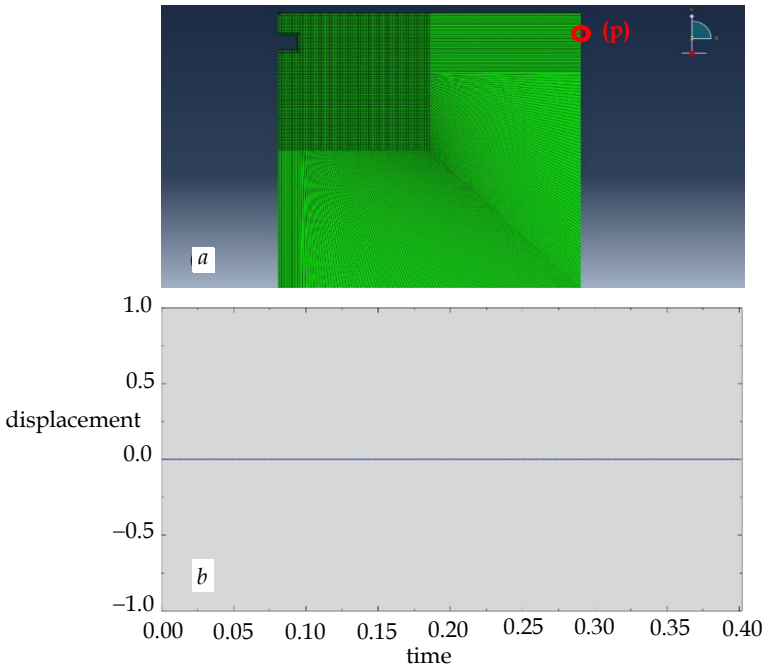

Figure 6. Displacements of a point in the infinite region for tunnel depth d_1 = 4 m and reinforcement case AS_{max} *. (a) selected point, (b) displacements of the selected point*

To validate whether the model soil boundaries are sufficiently far, the values of the maximum acceleration in the *y* direction were monitored at 7 points in the soil. Figure 7 shows the selected points and the maximum acceleration diagram. Table 5 shows the maximum values of the acceleration at these points.

It is observed that the dynamic load effect disappears with the distance to the tunnel, which indicates that the boundaries of the chosen soil field and its dimensions are sufficient to obtain correct and accurate results.

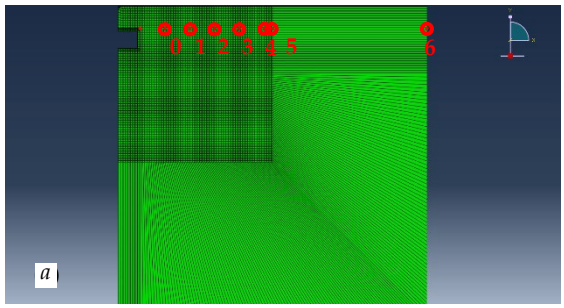

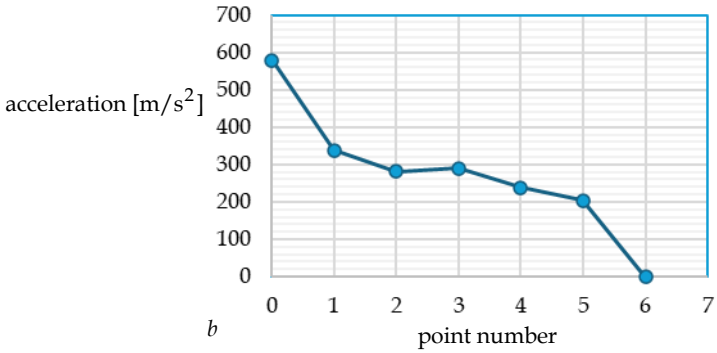

Figure 7. The soil maximum acceleration in the y direction at the selected points for tunnel depth d_1 = 4 m and reinforcement case AS_{max} . (a) point locations, (b) maximum acceleration diagram at the selected points

Table 5. Maximum values of the acceleration in the y direction of the selected points

point number	maximum acceleration *y* values [m/s²]
0	579.468
1	338.622
2	281.049
3	290.326
4	237.551
5	204.179
6	0

3.2 ***Propagation of induced blast waves in the soil***

The calibration of the direct blast waves in the soil is achieved on a set of target points that are selected on an inclined line at an angle of 45° to the ground surface. These target points are shown in Figure 2a [7, 10] and located to be remote from the effects of the free surface

and the boundary conditions [1, 7, 10]. The points have a distance to the detonation point of R = 0.9 to 5 m. The following empirical equation, adopted from design manual [1], is used to predict the blast pressure in the soil.

$$P_p = f\,A\,\rho_c \left(\frac{R}{W^{\frac{1}{3}}} \right)^{-n} \tag{2}$$

This previous equation can be rewritten as follows [7, 10].

$$P_p = c \left(\frac{R}{W^{\frac{1}{3}}} \right)^{-n} \tag{3}$$

where, R is the distance to the charge centre, W is the explosive mass, f is a coupling factor, A is a constant, ρ_c is the acoustic impedance, n is a constant attenuation factor, which depends on the soil properties [1, 5] and c is a constant that depends on the properties of soil and charge material [1]. In this paper, the constants adopted for this problem are adopted from [7, 10] and shown in Table 6. It is noted that many studies have re-examined the peak pressure in soils due to equation (2) [9, 13].

Table 6. Constants of the peak pressure equation

state	c	n
empirical upper limit [10]	1.12	2.75
empirical lower limit [10]	0.65	2.50
numerical results	1.14	2.17

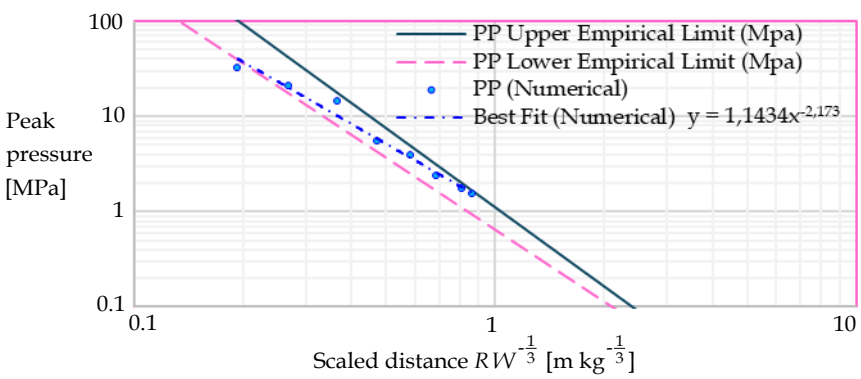

Figure 8. Free field calibration

Figure 8 shows the best-fit line of the numerical peak pressures due to the free field calibration. The values of the numerical constants are close enough to the limits of the experimental ones.

3.3 *Soil-tunnel interaction*

Figure 9 shows the interaction of the tunnel with the soil at the exact contact target points. The graph show the vertical displacements of the tunnel roof and that of the soil. It can be observed that the sliding contact separates and then rebounds again. The results show that this complete coupled numerical model can represent the dynamic response of the tunnel.

3.4 *Soil stresses validation*

To perform a validation of the stability of the soil around the tunnel, the peak Von Mises stresses are calculated along three paths (Fig. 10 and 11).

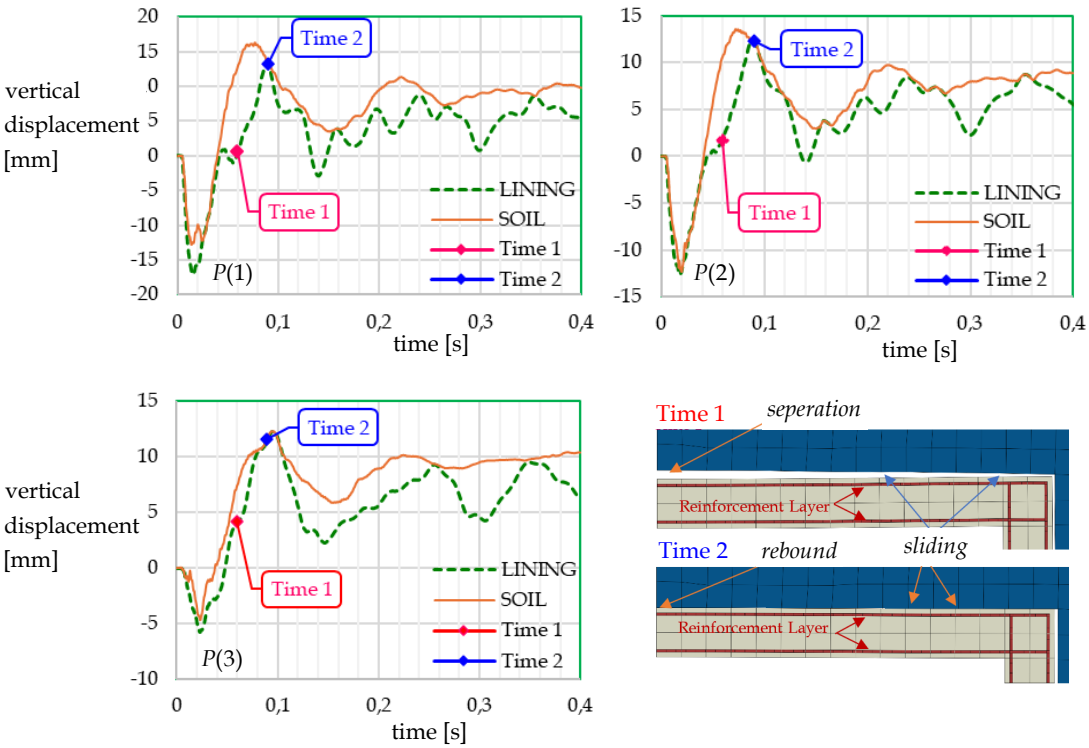

Figure 9. Interaction of the tunnel lining with the soil for structure depth d_1 = 4 m, and reinforcement case AS_{max} *. See Figure 10, for the locations of points P(1), P(2) and P(3).*

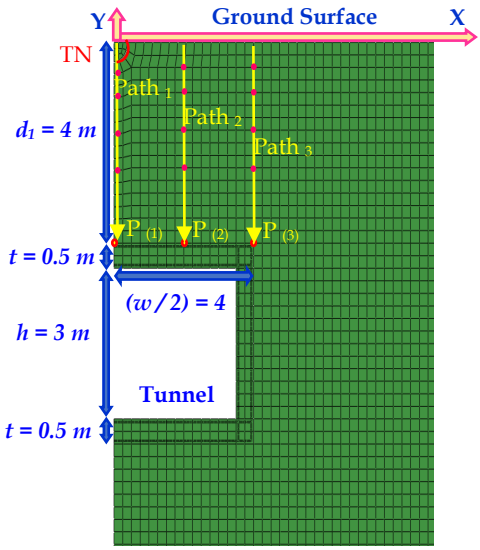

Figure 10. Validation of the stability of the soil around the tunnel lining roof

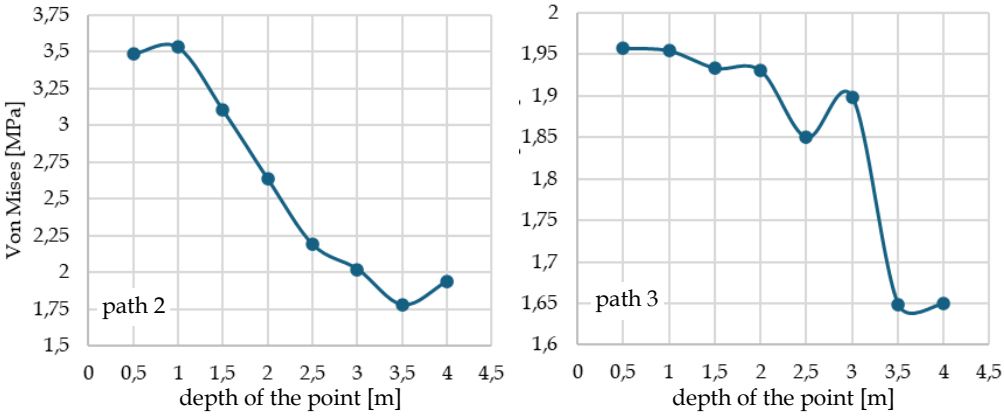

Figure 11. Von Mises stresses in the soil for three paths (d_1 , AS_{max})

The soil around the tunnel remains elastic because the stresses around the roof do not exceed the value of plastic soil stress 2.75 MPa (Table 2). Plastic deformation of the soil is confined to the area near the charge. The conclusion is that no collapse of soil occurs around the tunnel roof, which means there is no need to consider self-weight of collapsed soil as an additional static load after the explosion and the dynamic simulation is enough in this problem.

3.5 ***Structure response***

First, the reinforcement ratio of the lining is varied with constant depth of the tunnel d_1 = 4 m. Second, the tunnel depth is increased from d_1 = 4 m to d_2 = 8 m.

3.5.1 Effect of the reinforcement ratio

The reinforcement ratios lie between minimum and maximum values [2]. Figure 12 shows the vertical displacements at the three selected target points of the roof for all cases of reinforcement, using the tunnel depth of d_1 = 4 m. The results indicate that as the reinforcement ratio increases, the peak of the displacements reduces remarkably but

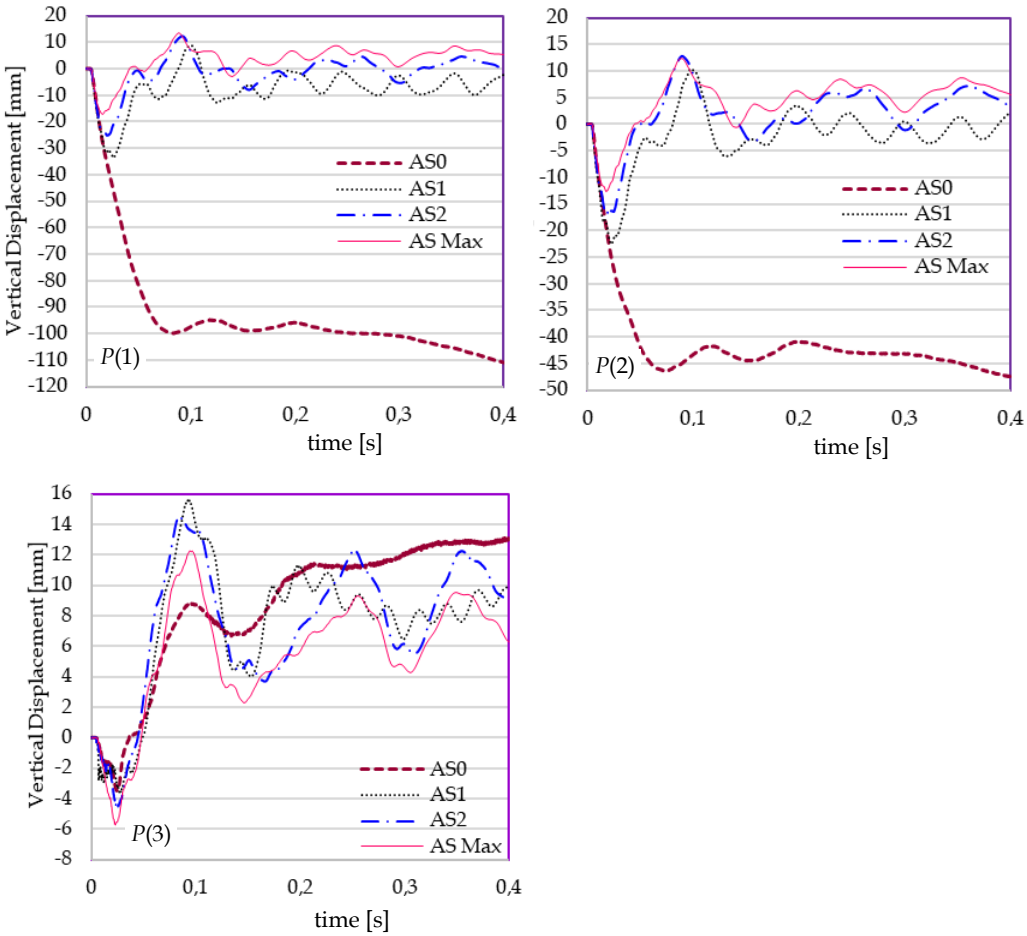

Figure 12. Vertical displacements of the tunnel roof; structure depth d_1 = 4 m

with final residual displacements. The same result was obtained for lateral displacements. The permanent displacement for case AS_0 is the largest in magnitude of about 111 mm for point 1 and about 47.5 mm for point 2, while for point 3 it is about 13.1 mm, which shows large damage or failure in the roof. In comparison, in the other reinforcement cases, the permanent displacement is not over 5 mm for points 1 and 2 and about 9 mm for point 3. The tunnel without reinforcement fails in a brittle way. The greatest expected damage occurs at point 1.

A damage index value equal to 1 means a complete loss of element strength, a value of 0 means that no damage occurs while a value of 0.7 means severe damage and the beginning of failure [8]. Figure 13 shows the damage to the concrete lining and Figure 14 shows the damage index at the target points of the roof at a tunnel depth d_1 = 4 m.

Figure 13 indicates the distribution of damage within the concrete lining with its parts (roof, wall and floor), unreinforced or reinforced with all reinforcement ratios. The concentration of severe damage in the reinforced concrete is evident with its greatest

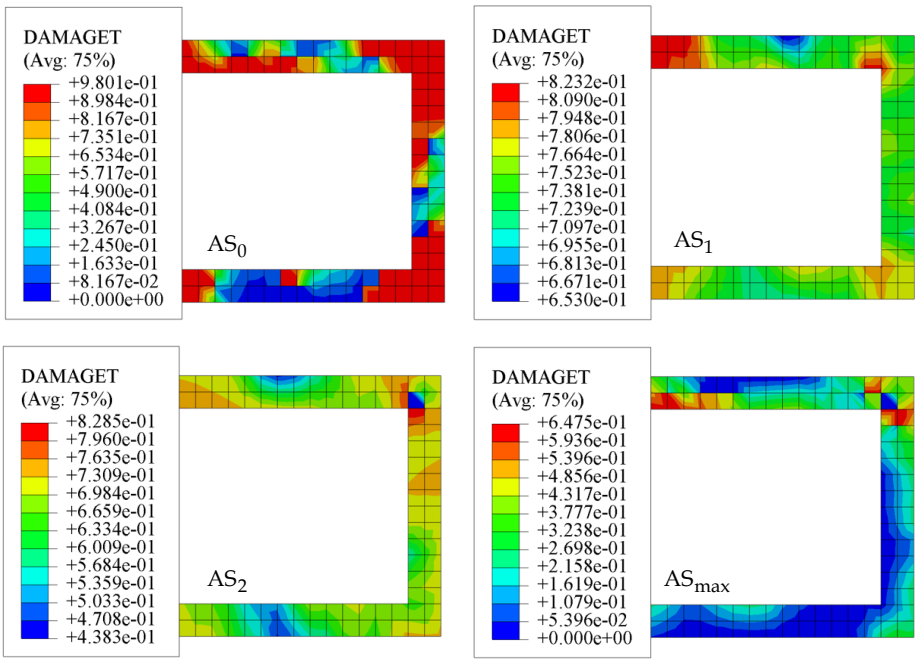

Figure 13. Damage of the concrete lining; structure depth d_1 = 4 m; four reinforcement cases

values at the centre of the roof and at the roof-wall joint. Relatively large damage occurs at the reinforcement ratios AS_1 and AS_2 with lower values of damage at the maximum reinforcement ratio AS_{max} . The damage is severe in case of no reinforcement AS_0 .

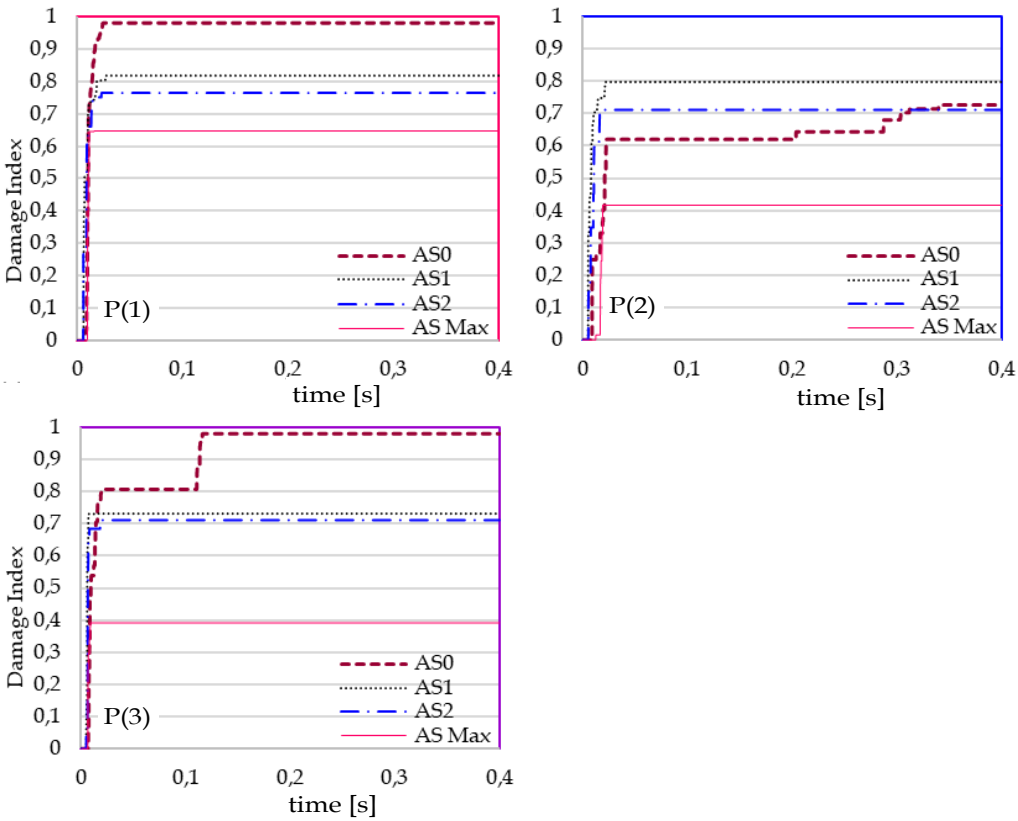

Figure 14. Damage index at the target points of the lining roof. Structure depth d_1 = 4 m

The previous values of the damage index can be interpreted as follows: Significant damage and the beginning of collapse of the lining occurs in target points of the roof at the reinforcement ratios AS_0 , AS_1 and AS_2 due to the value of the damage index exceeding the standard value 0.7, especially if static loads are taken into account. The damage is within acceptable limits when using the maximum reinforcement ratio AS_{max} . It is clear that the damage index decreases by increasing the ratio of reinforcement, this can be explained by the contribution of the reinforcement layer in increasing the capacity of the structural element.

3.5.2 *Effect of tunnel depth*

Figure 15 shows the vertical displacements of the centre of the roof at each considered reinforcement ratio with changing depth of the tunnel ($d_1 \sim d_2 = 2\,d_1$). It is clear from the figure that increasing the tunnel depth significantly reduces the value of the peak vertical displacements, with a ratio estimated at 79% for case AS_0 , 67% for case AS_1 and about 55% for cases AS_2 and AS_{max} . There are still residual final displacements. The same results occur in the lateral displacements, but with a slightly different reduction ratio. The damage evaluation has been also done for the tunnel depth d_2 = 8 m as shown in Figure 16.

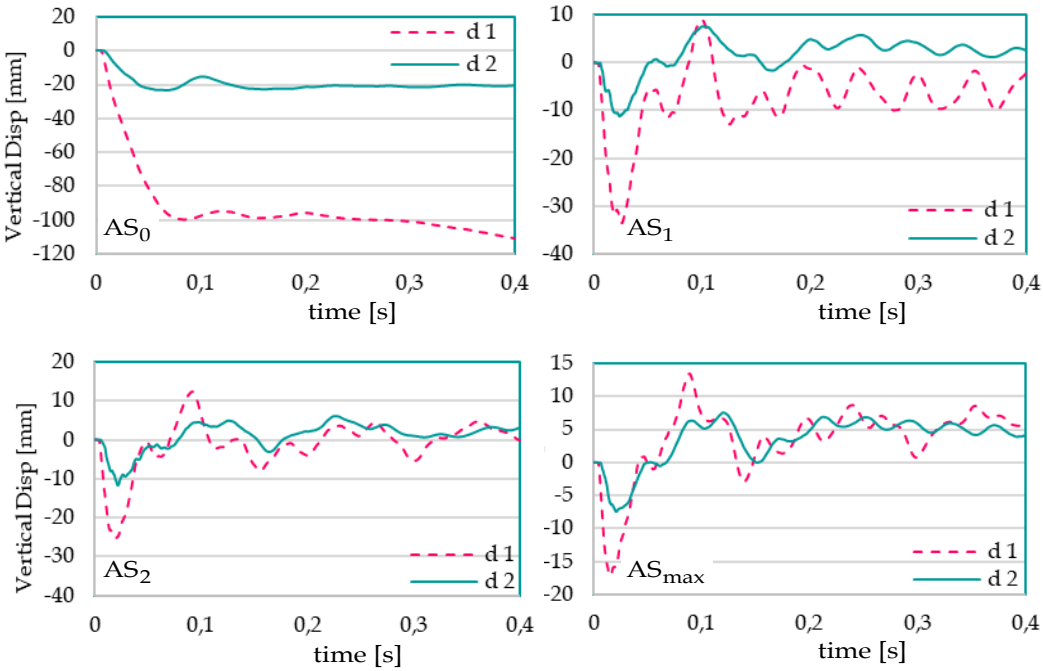

Figure 15. Vertical displacements at point (1). Depth of structure (d_1 = 4 m and d_2 = 8 m), and four reinforcement cases

At this depth, in case of an unreinforced lining AS_0 , there is damage to the roof, concentrated in its centre as well as in the corner, with relative damage to the wall, even though there is no reinforcing layer connecting the structural elements. This may be caused by the relatively large depth. Therefore, even though this case AS_0 is hypothetical, the effect of the small explosive is a joint action of the elements and subsequently the complete collapse in the centre and the corner of the roof. The distribution of damage at this depth is

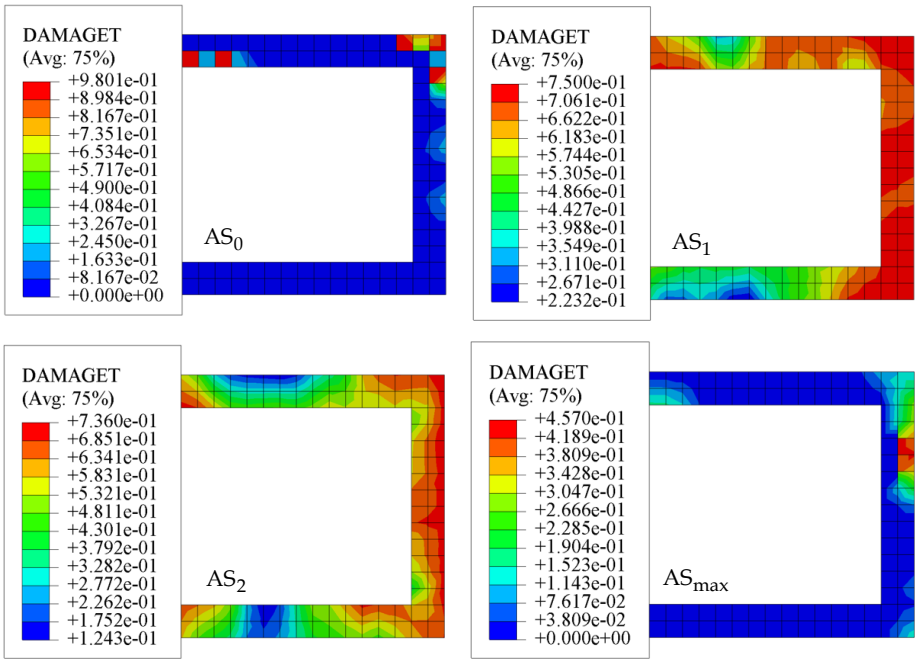

Figure 16. Damage in the concrete lining; tunnel depth d_2 = 8 m; for four reinforcement cases

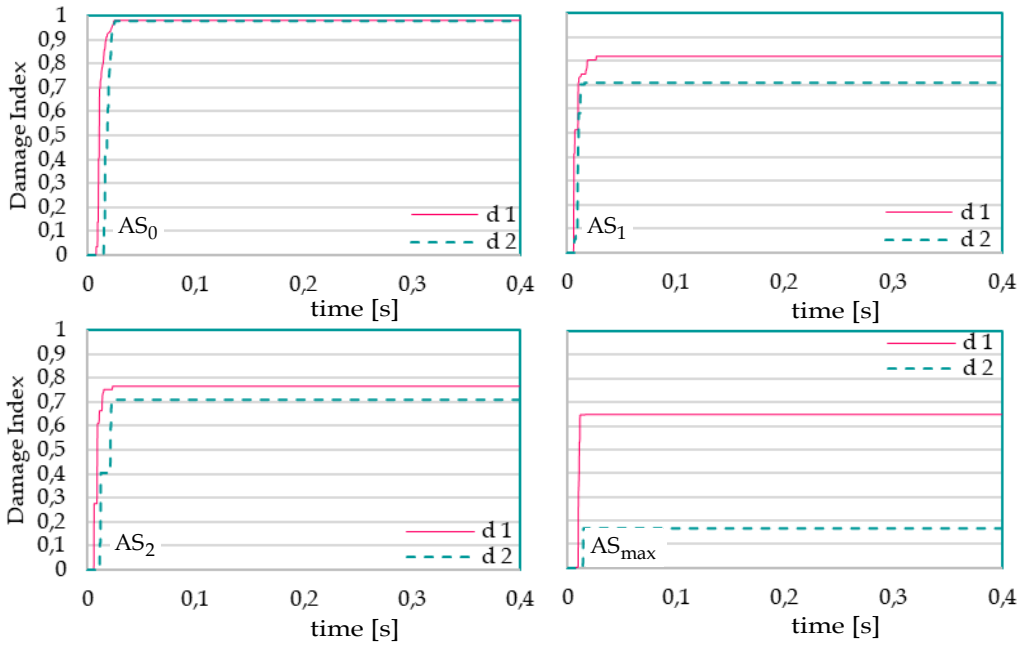

Figure 17. Damage index of the concrete lining at point (1). Structure depth d_1 = 4 m and d_2 = 8 m and four reinforcement cases

almost similar to that at the previous small depth for the reinforcement ratios AS_1 and AS_2. The largest values of damage are in the roof centre as well as the lining walls, with little damage in the floor. Little damage occurs for the maximum reinforcement ratio case AS_{max}, in the roof centre with greater damage appearing in the walls. Figure 17 exhibits the damage index at the centre of the roof concerning different reinforcement ratios and depths as an example.

By increasing the tunnel depth, the roof is still damaged and begins to collapse at the roof for cases AS_0, AS_1 and AS_2. An additional collapsed area occurs at the lining wall and floor, where the damage index values are over the standard value 0.7, especially if static loads are taken into account. The lining with the maximum reinforcement ratio AS_{max} is safe with limited damage.

4 Conclusion

The following conclusions can be drawn from the investigation presented in this paper.

- The peak in vertical and horizontal displacements of the tunnel roof decreases by increasing the reinforcement ratio of the tunnel lining, however, the permanent deformation increases.
- As the reinforcement ratio increases to the maximum value, the damage index decreases proportionally.
- As the tunnel depth of doubles, the peak of vertical and lateral displacements decreases remarkably but not proportionally.
- It is beneficial to have severely damaged areas outside the expected most critical areas.
- An optimum tunnel design can be achieved, considering acceptable damage and a safe facility, by choosing an appropriate reinforcement ratio and tunnel depth.

References

[1] Anonymous (1986). Fundamentals of protective design for conventional weapons (TM 5-855-1). Technical manual, US Department of Army, Vicksburg U.S.A. Online: https://www.nrc.gov/docs/ML1019/ML101970069.pdf

[2] Anonymous (2004). Syrian Earthquake Building Code, Syrian engineering association publications. Damascus, Syria (in Arabic)

[3] Anonymous (2014). ABAQUS/Standard User's Manual, Version 6.14. Dassault Systèmes, Paris, Online: http://62.108.178.35:2080/v6.14/index.html

[4] Anonymous (2018). Guideline for design of road tunnel. Technical assistance for improvement of capacity for planning of road tunnels, Japan and Sri Lanka, Japan International Cooperation Agency (JICA), Road Development Agency (RDA), Sri Lanka, Online: https://openjicareport.jica.go.jp/pdf/12303566.pdf

[5] Bulson, P. S. (1997). *Explosive loading of engineering structures*. CRC Press.

[6] Hu, Y., & Randolph, M. F. (1998). A practical numerical approach for large deformation problems in soil. *International Journal for Numerical and Analytical Methods in Geomechanics*, 22(5), 327-350.

[7] Khadra, A. A., Hasan, H., Tabak, T., & Hammoud, I. (2023). Dynamic behavior of buried structures under the effect of surface explosions using nonlinear numerical modelling. *Damascus University Journal for The Engineering Sciences*,

[8] Kim, T. H., Lee, K. M., Chung, Y. S., & Shin, H. M. (2005). Seismic damage assessment of reinforced concrete bridge columns. *Engineering Structures*, 27(4), 576-592.

[9] Leong, E. C., Anand, S., Cheong, H. K., & Lim, C. H. (2007). Re-examination of peak stress and scaled distance due to ground shock. *International Journal of Impact Engineering*, 34(9), 1487-1499.

[10] Nagy, N., Mohamed, M., & Boot, J. C. (2010). Nonlinear numerical modelling for the effects of surface explosions on buried reinforced concrete structures. *Geomechanics and Engineering*, 2(1), 1-18.

[11] Nagy, N. M. (2015). Numerical Evaluation of Craters Produced by Explosions on the Soil Surface. *Acta Physica Polonica*, A., 128.

[12] Yang, Y., Xie, X., & Wang, R. (2010). Numerical simulation of dynamic response of operating metro tunnel induced by ground explosion. *Journal of Rock Mechanics and Geotechnical Engineering*, 2(4), 373-384.

[13] Yankelevsky, D. Z., Karinski, Y. S., & Feldgun, V. R. (2011). Re-examination of the shock wave's peak pressure attenuation in soils. *International Journal of Impact Engineering*, 38(11), 864-881.